Non-Orthogonal-to-the-Flow Electric Field Improves Resolution in the Orthogonal Direction: Hidden Reserves for Combining Synthesis and Purification in Continuous Flow

ARTICLE *in* ANALYTICAL CHEMISTRY · FEBRUARY 2010

Impact Factor: 5.64 · DOI: 10.1021/ac902546y · Source: PubMed

3 AUTHORS, INCLUDING:

Victor Okhonin
Custoiometrics Inc.
68 PUBLICATIONS **827** CITATIONS
SEE PROFILE

Sergey N Krylov
York University
167 PUBLICATIONS **3,625** CITATIONS
SEE PROFILE

Anal. Chem. **2010,** *82,* 1183–1185

Letters to *Analytical Chemistry*

Non-Orthogonal-to-the-Flow Electric Field Improves Resolution in the Orthogonal Direction: Hidden Reserves for Combining Synthesis and Purification in Continuous Flow

Victor Okhonin, Christopher J. Evenhuis, and Sergey N. Krylov*

Department of Chemistry and Centre for Research on Biomolecular Interactions, York University, Toronto, Ontario M3J 1P3, Canada

There is a pressing need for continuous purification of products of synthesis conducted in continuous-flow microreactors. An existing technique, micro free-flow electrophoresis (μFFE), could fulfill this niche if its resolving power for similar molecules was improved. MicroFFE continuously separates ions in the hydrodynamic flow by an electric field orthogonal to the flow. Here, we prove theoretically from first principles that the resolving power of μFFE can be greatly improved by the use of a nonorthogonal to the flow field. This result may be decisive in starting practical attempts to combine synthesis in continuous-flow microreactors with continuous-flow purification by μFFE.

The advantages of chemical synthesis in continuous-flow microreactors over synthesis in conventional batch reactors make it highly attractive for many synthetic applications.[1] To exploit fully these advantages, continuous-flow microsynthesis of products should be followed by their continuous-flow micropurification.[1] To the best of our knowledge, such a combination has not yet been developed. Continuous-flow micropurification can be achieved if a microreactor exits into a wide micropurification channel in which products are separated in the direction orthogonal to the flow and continuously collected at the exit of the channel. This work was motivated by our insight that an existing continuous-flow micropurification technique, microfree flow electrophoresis (μFFE), is naturally suited for being combined with continuous-flow microsynthesis. μFFE facilitates continuous separation of molecules in a wide microchannel with a hydrodynamic flow between two open ends and an electrical field orthogonal to the flow (Figure 1A).[2] μFFE has, however, a limited resolving power for species with similar charge-to-size ratios, which limits its practical applicability to combined microsynthesis/micropurification.[3] Here, we report on (i) the development of a general theory of μFFE from first principles (from mass- and heat-transfer equations) and (ii) our finding from the theory that a nonorthogonal electrical field can greatly improve resolution of difficult-to-separate species in the orthogonal direction (Figure 1B). The latter effect is somewhat counterintuitive and was overlooked in all previous works. Our results suggest that μFFE has unexplored reserves in improving its separating power and can potentially be a

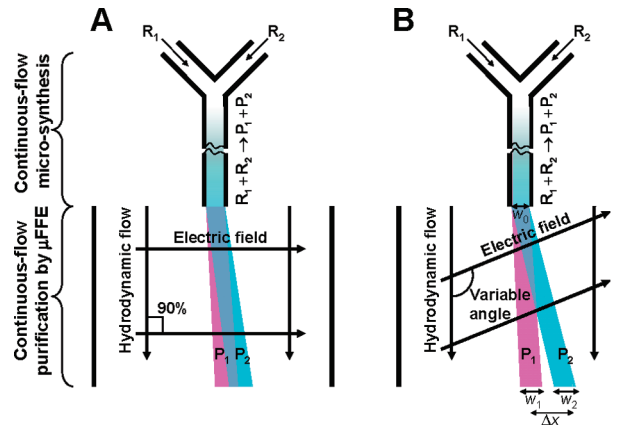

Figure 1. Schematic representation of separation of products P_1 and P_2 in an integrated system for in-flow microsynthesis followed by micropurification by μFFE with orthogonal (A) and nonorthogonal (B) orientations of the electric field and hydrodynamic flow.

* To whom correspondence should be addressed. E-mail: skrylov@yorku.ca.

(1) (a) Wiles, C.; Watts, P. *Eur. J. Org. Chem.* **2008**, *10*, 1655–1671. (b) Gustafsson, T.; Gilmour, R.; Seeberger, P. H. *Chem. Commun.* **2008**, 3022–3024. (c) Hartung, A.; Keane, M. A.; Kraft, A. *J. Org. Chem.* **2007**, *72*, 10235–10238. (d) Geyer, K.; Codee, J. D. C.; Seeberger, P. H. *Chem.—Eur. J.* **2006**, *12*, 8434–8442.

(2) Raymond, D. E.; Manz, A.; Wldmer, H. M. *Anal. Chem.* **1994**, *66*, 2858–2865.

(3) (a) Hannig, K.; Wirth, H.; Meyer, B.-H.; Zeiller, K. *H.-S. Z. Physiol. Chem.* **1975**, *356*, 1209–1223. (b) Raymond, D. E.; Manz, A.; Widmer, H. M. *Anal. Chem.* **1996**, *68*, 2515–2522. (c) Kašička, V. *Electrophoresis* **2009**, *30*, S40–S52.

(4) (a) Kohlheyer, D.; Eijkel, J. C. T.; van den Berg, A.; Schasfoort, R. B. M. *Electrophoresis* **2008**, *29*, 977–993. (b) Fonslow, B. R.; Bowser, M. T. *Anal. Chem.* **2006**, *78*, 8236–8244. (c) Klepárník, K.; Otevrel, M. *Electrophoresis* **2004**, *25*, 3633–3642. (d) Raymond, D. E.; Manz, A.; Widmer, H. M. *Anal. Chem.* **1996**, *68*, 2515–2522. (e) Fonslow, B. R.; Bowser, M. T. *Anal. Chem.* **2008**, *80*, 3182–3189.

(5) (a) Aris, R. *Proc. R. Soc. London, Ser. A* **1956**, *A235*, 67–77. (b) Ravoo, E.; Gellings, P. J.; Vermeulen, T. *Anal. Chim. Acta* **1967**, *38*, 219–232.

10.1021/ac902546y
Published on Web 01/21/2010

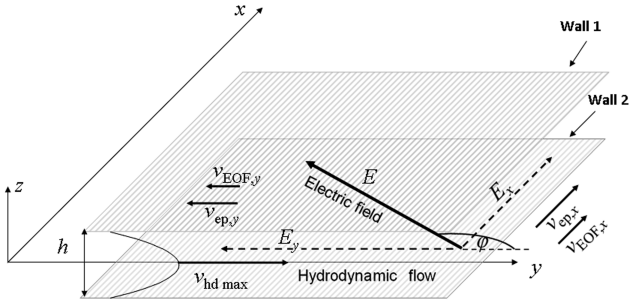

Figure 2. Schematic diagram of μFFE's defining geometry used in the development of its general theory (see the text for details). Our consideration also includes two side walls in the $z-y$ planes which are not shown in the figure. The side walls physically limit the z size of the flow chamber, making the chamber geometry similar to that of a practical μFFE device.

practical approach for continuous-flow micropurification following continuous-flow microsynthesis.

RESULTS AND DISCUSSION

Despite a considerable body of theoretical works on μFFE,[4] a theory of μFFE has never been derived from first principles, which could potentially lead to mistakes. Moreover, all theoretical works considered only the orthogonal electric filed (Figure 1A), intuitively assuming that it is optimal for separation. The aim of this work was to derive a general theory of μFFE from first principles. To generalize the theory, we considered all possible field orientations in the plane of the hydrodynamic flow (Figure 1B).

The final goal of our work was to derive a general expression for resolution, R_S, of species 1 and 2 in the orthogonal direction which is defined as

$$R_S = 2\Delta x/(w_1 + w_2) \tag{1}$$

where Δx is the distance between stream centers of the two species and w_1 and w_2 are the widths of the streams in the orthogonal direction (Figure 1B). We consider the following general theoretical setup of μFFE (Figure 2). A thin channel has two walls in the $x-y$ plane separated by a distance h. The hydrodynamic flow, between the walls and in the y direction, has its maximum velocity of $v_{hd\ max}$ in the plane equidistant from the two walls ($z = 0$). The friction of the fluid against the walls creates a parabolic flow profile in the $y-z$ plane. An electric field in the $x-y$ plane makes an angle φ with the direction of the hydrodynamic flow. The electric field is assumed to be uniform with a constant strength E projected on axes x and y as E_x and E_y, respectively. The projections of the electric field on x and y cause electroosmotic flow in both directions with velocity components of $v_{EOF,x}$ and $v_{EOF,y}$, respectively. A charged molecule placed in the electric field and in a conducting fluid (electrolyte) will experience a combination of an electrostatic force and a frictional force, which leads to an electrophoretic motion with a constant electrophoretic velocity, v_{ep}, parallel to E. This velocity has projections $v_{ep,x}$ and $v_{ep,y}$ on axes x and y, respectively.

When a stream of molecules is introduced into the channel with the electrolyte and the electric field, their mass transport will be defined by their electrophoretic motion, diffusion, and adsorption/desorption on the walls as well as by hydrodynamic and electroosmotic flows. The electric field in the electrolyte generates an electric current and produces heat. To realize a general theory of μFFE, we must solve both the mass-transport and heat-transfer equations, taking into account variations in hydrodynamic flow, electrophoretic motion, and diffusion coefficient caused by fluid friction against the walls and the finite rate of heat dissipation. These variations are partly due to temperature dependence of fluid viscosity and only occur in the z direction due to the translational symmetry in the $x-y$ plane.

The equations for mass transport and heat transfer are[5]

$$\frac{\partial c}{\partial t} = -\frac{\partial v_x c}{\partial x} - \frac{\partial v_y c}{\partial y} + \frac{\partial}{\partial x}D\frac{\partial c}{\partial x} + \frac{\partial}{\partial y}D\frac{\partial c}{\partial y} + \frac{\partial}{\partial z}D\frac{\partial c}{\partial z} \tag{2}$$

$$\lambda\left(\frac{\partial^2 T}{\partial x^2} + \frac{\partial^2 T}{\partial z^2}\right) - \rho C_p\frac{\partial T}{\partial t} + \kappa E^2 = 0 \tag{3}$$

where c is the molecular concentration, t is the time, v_x and v_y are the x and y components of the resultant velocity, D is the diffusion coefficient and, finally, λ, T, ρ, C_p, and κ are the thermal conductivity, temperature, density, specific heat capacity, and electrical conductivity of the electrolyte. To obtain expressions for the lateral separation, Δx, and widths of the separated streams, w, we solved eq 2 from first principles using a set of boundary conditions and assumptions and used a known approximation for $\Delta T(z)$ as the solution for eq 3[5b] (see Supporting Information). Substitution of the expressions for Δx and w into eq 1 results in a general equation for resolution (eq 4.20 in Supporting Information). For small variations in temperature, our general expression for resolution simplifies to

$$R_S = \frac{\left|\dfrac{(\mu_{ep1}-\mu_{ep2})LE\sin\varphi(\mu_{EOF}E\cos\varphi+\bar{v}_{hd})}{\{(\mu_{EOF}+\mu_{ep1})E\cos\varphi+\bar{v}_{hd}\}\{(\mu_{EOF}+\mu_{ep2})E\cos\varphi+\bar{v}_{hd}\}}\right|}{2\left(\sqrt{\dfrac{w_0^2}{12}+\dfrac{2L}{(\mu_{EOF}+\mu_{ep1})E\cos\varphi+\bar{v}_{hd}}\left(\dfrac{h^2E^2\sin^2\varphi}{210D_1}\left(\mu_{EOF}+\dfrac{\mu_{ep1}\bar{v}_{hd}}{(\mu_{EOF}+\mu_{ep1})E\cos\varphi+\bar{v}_{hd}}\right)^2\right.\right.}\right.} \\ \left.\left.+D_1\left(1+\left(\dfrac{\mu_{ep1}E\sin\varphi}{(\mu_{EOF}+\mu_{ep1})E\cos\varphi+\bar{v}_{hd}}\right)^2\right)\right)+ \\ \sqrt{\dfrac{w_0^2}{12}+\dfrac{2L}{(\mu_{EOF}+\mu_{ep2})E\cos\varphi+\bar{v}_{hd}}\left(\dfrac{h^2E^2\sin^2\varphi}{210D_2}\left(\mu_{EOF}+\dfrac{\mu_{ep2}\bar{v}_{hd}}{(\mu_{EOF}+\mu_{ep2})E\cos\varphi+\bar{v}_{hd}}\right)^2\right.} \\ \left.\left.+D_2\left(1+\left(\dfrac{\mu_{ep2}E\sin\varphi}{(\mu_{EOF}+\mu_{ep2})E\cos\varphi+\bar{v}_{hd}}\right)^2\right)\right)\right) \tag{4}$$

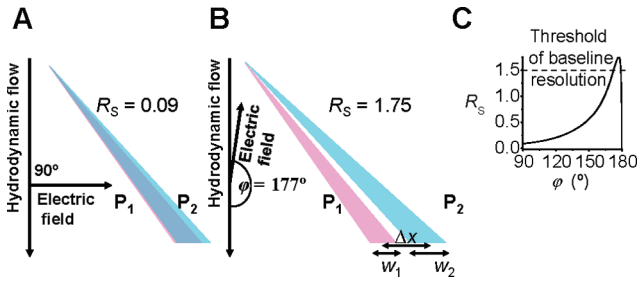

Figure 3. Computer simulated separation of two molecules with MW difference of 1.4% (difference equivalent to one CH_2 group in a 1 kDa molecule) in orthogonal (A) and nonorthogonal μFFE (B) with identical strength of the electric field. The calculated electrophoretic mobilities were $\mu_{ep1} = 2.753 \times 10^{-8}$ and $\mu_{ep2} = 2.766 \times 10^{-8}$ $m^2s^{-1}V^{-1}$. The hydrodynamic flows for the separation of the products were adjusted ($\bar{v}_{hd} = 6.21 \times 10^{-5}$ ms^{-1} in panel A and $\bar{v}_{hd} = 5.60 \times 10^{-4}$ ms^{-1} in panel B) so that the average widths of the streams after separation would be the same. The electrical field strength was the same in both panels, $E = 2.0 \times 10^4$ Vm^{-1}, but the angle, φ, was different: $\varphi = 90°$ in panel A and $\varphi = 177°$ in panel B. The height of the separation channel was assumed to be 20 μm for both panels. Panel C shows variation of resolution with the angle φ between the hydrodynamic flow and the electrical field.

where $\bar{v}_{hd}$ is the average hydrodynamic velocity, L is the length of the separation channel, μ_{ep} is the electrophoretic mobility ($= v_{ep}/E$), μ_{EOF} is the electroosmotic mobility ($= v_{EOF}/E$), w_0 is the initial width of the stream of non-separated species and the angle φ is between the directions of the hydrodynamic flow and the electric field (see Figure 2). Subscripts 1 and 2 refer to the separated species 1 and 2.

Intuitively, the best resolution of the species in the orthogonal direction can be obtained with φ equal to 90°. The analysis of eq 4, however, suggests that this assumption is incorrect: the resolution can be markedly better for φ different from 90° with the same field strength if $(\mu_{EOF} + \mu_{ep1})E\cos\varphi + \bar{v}_{hd}$ is much smaller than $\bar{v}_{hd}$and greater than zero. Figure 3 shows the dependence of R_S on φ calculated using eq 4 for two difficult to separate molecules. These molecules cannot be baseline separated by the orthogonal electric field but can be by a nonorthogonal field.

While the improved resolution in the orthogonal direction with the nonorthogonal field is counterintuitive at the first glance, in retrospect, it can be explained without referring to eq 4. Indeed, if φ is chosen so that the electrophoretic velocities have projections against the hydrodynamic flow, then the separated molecules are retained longer in the field. The longer retention would not result in a significant resolution improvement if it were identical for the two molecules. In the nonorthogonal field, however, the molecule with the greater electrophoretic velocity is retained longer than the one with the lower velocity and is, thus, deflected further in the orthogonal direction. The differential retention mechanism of resolution improvement in μFFE can only be achieved with a nonorthogonal field.

Our analysis of eq 4 shows that improved resolution with a nonorthogonal field is possible due to a greater gain in lateral separation, Δx, than an increase of the widths, w, of the separated streams. The general theory also reveals that an important phenomenon, namely diffusion in the direction of the hydrodynamic flow, was previously overlooked, which underestimates band broadening (see Supporting Information).

CONCLUDING REMARKS

To conclude, the general theory of μFFE suggests that there is a previously unknown and, thus, unexplored means of markedly improving its resolving power: nonorthogonal orientation of the electric field to the hydrodynamic flow. With this new feature and its scale suitability, μFFE may be the best candidate for combining continuous-flow microsynthesis with continuous-flow micropurification. Further studies will be needed to (i) develop approaches for optimizing parameters in μFFE, (ii) prove the principle of nonorthogonal μFFE experimentally, and (iii) verify the practicality of the tandem of continuous-flow microsynthesis and micropurification. The general theory of FFE presented here will serve as an indispensable tool in such studies.

ACKNOWLEDGMENT

This work was funded by Natural Sciences and Engineering Research Council of Canada. We thank Dr. L. Cherney (University of Alberta) for carefully reading the manuscript and providing very useful comments.

SUPPORTING INFORMATION AVAILABLE

Supporting (i) solution of mass transport equation, (ii) derivation of expression for resolution, (iii) comparison of new and previous expressions for resolution, and (iv) conditions used for computer simulations in Figure 3. This material is available free of charge via the Internet at http://pubs.acs.org.

Received for review November 6, 2009. Accepted December 20, 2009.

AC902546Y

SUPPORTING INFORMATION

Non-Orthogonal-to-the-Flow Field Improves Resolution in the Orthogonal Direction: Hidden Reserves for Combining Synthesis and Purification in Continuous Flow

Victor Okhonin, Christopher J. Evenhuis, and Sergey N. Krylov*

Department of Chemistry and Centre for Research on Biomolecular Interactions, York University, Toronto, Ontario M3J 1P3, Canada

Table of Contents

Page number

Assignments……... S2

I. Solution of the mass-transport equation (Eq. (2) in manuscript) for micro free flow electrophoresis (μFFE)……..... S4

1. Two-dimensional equations describing mass transfer for arbitrary velocity profiles…….... S4

2. General expression for peak broadening……. S7

3. Determination of the velocity profiles……. S9

II. Derivation of a general equation for resolution, R_S…….. S14

III. Comparison with previous expressions for resolution……. S18

IV. Conditions used in computer simulations in Figure 3 in main text……. S19

References…….. S19

Assignments

α_η – temperature coefficient for dynamic viscosity (K^{-1})

α_D – temperature coefficient for diffusion coefficient (K^{-1})

α_μ – temperature coefficient for electrophoretic mobility (K^{-1})

β – defined parameter that describes non-stationary dispersion due to adsorption

γ – matrix parameter associated with diffusion in the x and y directions

Γ – defined paramter that describe the maximum fractional change to D due to temperature effects

$\delta c(x,y,z,t) \equiv c(x,y,z,t) - \overline{c}(x,y,t)$ (M)

$\delta v_{\text{buf,x}}(z) \equiv v_{\text{buf,x}}(z) - \overline{v}_{\text{buf,x}}$ describes variation of electrolyte velocity from the mean value in the x direction

$\delta v_{\text{buf,y}}(z) \equiv v_{\text{buf,x}}(z) - \overline{v}_{\text{buf,x}}$ describes variation of electrolyte velocity from the mean value in the y direction

δv_x, δv_y – variation of product stream velocities from the mean values in the x or y directions, respectively

$\delta D \equiv D(z) - \overline{D}$ ($m^2 s^{-1}$)

$\Delta T(z)$ – difference in temperature between wall and the electrolyte at depth, z (K)

ε – electrical permitivity of the medium (Fm^{-1})

ζ – zeta potential of upper and lower wall (V)

η – dynamic viscosity of the electrolyte (Pa s)

θ – dimensionless position in the z direction ($= 2z / h$)

Θ – defined parameter that describes dispersion

κ – electrical conductivity of the electrolyte (Sm^{-1})

λ – thermal conductivity of the electrolyte ($Wm^{-1}K^{-1}$)

Λ – defined parameter that describes the maximum fractional change in viscosity due to temperature effects

μ_{ep} – electrophoretic mobility ($m^2 s^{-1} V^{-1}$)

μ_{EOF} – electroosmotic mobility ($m^2 s^{-1} V^{-1}$)

ρ – density of the electrolyte (kgm^{-3})

σ – standard deviation of a stream ($= \frac{1}{4} w$)

σ^2_x – variance in the direction perpendicular to the hydrodynamic flow (m^2)

Σ – sum

τ – defined paramter that describes hydrodynamic dispersion

Υ – defined paramter that describes hydrodynamic velocity at the centre of the channel without heating effects

φ – angle between electric field vector and hydrodynamic flow (º)

Φ – defined parameter used to calculate higher moments of concentration distributions

χ_0, χ_1 – defined parameters used for the simplification of some expressions

ψ – defined paramter that describes the variation of the diffusion coefficient in the z direction

ω – defined paramter that describes the injection window with symmetry of velocity about $z = 0$

Ω – defined parameter that describes assymetry of the distributions

$a_+(x, y, t)$ – concentration of adsorbed solute at upper wall, as a function of coordinates x, y and time t (M)

$a_-(x, y, t)$ – concentration of adsorbed solute at unner wall, as a function of coordinates x, y and time t (M)

$c(x, y, z, t)$ – concentration of solute, as a function of coordinates x, y, z and time t (M)

$\overline{c}(x, y, t)$ – concentration of solute averaged in the z direction, as a function of coordinates x, y and time t (M)

D – diffusion coefficient (m^2s^{-1})

$\overline{D}$ – diffusion coefficient averaged in the z direction (m^2s^{-1})

E_x, E_y – components of the electric field in the x and y directions (Vm^{-1})

f, g – paramters which may be x or y

h – depth of the channel measured in the z direction (m)

J_x, J_y – average values of $v_x \delta c$ and $v_y \delta c$, respectively, calculated for values of z from $z = -h/2$ to $z = +h/2$

k_{ad} – coefficient (rate constant) of walls adsorption (ms^{-1})

k_{de} – coefficient (rate constant) of walls desorption (s^{-1})

L – length of separation channel (m)

$\hat{L}$ – defined operator

M – moments (these are functions of time)

p – pressure (Pa)

P – defined parameter that describes the maximum fractional change to the electrophoretic mobility due to temperature effects

q – charge on analyte ion (C)

r_h – hydrodynamic radius of solvated ion

s – coordinate system that describes position in the direction of the product streams

SLC – standard laboratory conditions, T = 298 K, p = 101.3 kPa

T_0 – temperature of the walls at $z = \pm h/2$ (K)

$v_{buf,x}(z)$, $v_{buf,y}(z)$ – total electrolyte velocities in the x and y directions as a function of z (= sum of hydrodynamic and electroosmotic velocities)

$v_{ep,x}$, $v_{ep,y}$ – x and y components of the electrophoretic velocity (ms^{-1})

$\overline{v}_{hd}$ – average velocity of hydrodynamic flow (in the y direction), averaged in the z-direction (ms^{-1})

$\tilde{v}_{hd,g}$ – constant of integration

$v_{hd\,max}$ – maximum velocity of hydrodynamic flow in the y direction (ms^{-1})

v_x, v_y – x and y components of the product resultant velocity (ms^{-1})

$\overline{v}_x$, $\overline{v}_y$ – x and y components of the product resultant velocity, averaged in the z direction (ms^{-1})

w_0 – width of introduced stream at point of injection (m)

w_1, w_2 – width of separated streams at points of collection

z', z'' – parameters for integration in the z direction.

I. Solution of the mass-transport equation (Eq. (2) in manuscript) for micro free flow electrophoresis (μFFE)

Our solution to the mass-transport equation is in three parts. Firstly, we convert the most general three-dimensional equation into a two-dimensional form by averaging in the *z* direction. Secondly, we derive an expression for variance in the *x* direction which is dependent on the velocity profile of the electrolyte and separated streams. Thirdly, we derive equations for the velocity profiles in the *x* and *y* directions.

1. Two -dimensional equations describing mass transfer for arbitrary velocity profiles

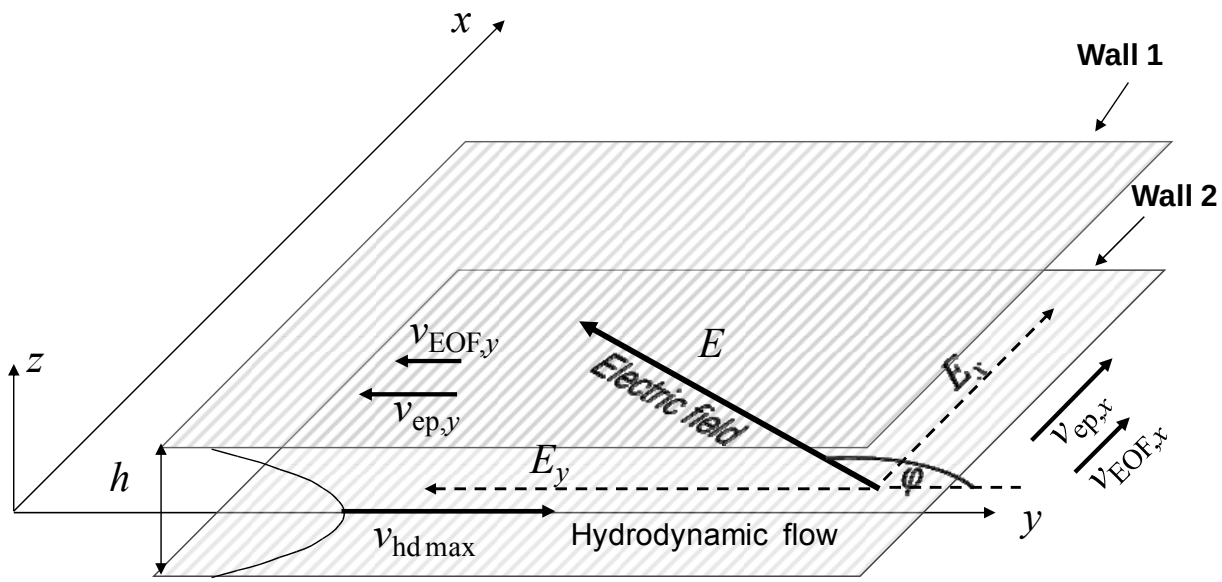

Figure S-1: Schematic diagram of μFFE's defining geometry used in the general theory development. To be more relevant to practical μFFE, our consideration also includes two side walls in the *z*-*y* planes which are not shown in the figure. These walls physically limit the size of the flow chamber in the *x* direction.

Taylor was the first to discuss dispersion in cylindrical pipes.[1] Later Aris extended this work to include rectangular channels.[2] To obtain the equation for the variation of concentration over time, we follow an approach similar to that of Aris to generalise Taylor's approach to dispersion in flat channels. Our approach is different to that of Aris, in that it also considers diffusional dispersion associated with migration in the electrical field. If hydrodynamic flow is along the *y* (as shown above in **Fig. S-1**), then the velocity of the flow is dependent on the distance from the central plane,[3] $z = 0$, and the other coordinates *x* and *y*. It is assumed that there is no flow in the *z* direction and that the *x* and *y* components of the product and molecules velocities are of the form:

$$v_x(x,y,z), \quad v_y(x,y,z), \quad v_z = 0$$

In μFFE, the precise equation to describe mass transport considers convection and diffusion; it has the form:

$$\frac{\partial c}{\partial t} = -\frac{\partial v_x c}{\partial x} - \frac{\partial v_y c}{\partial y} + \frac{\partial}{\partial x} D \frac{\partial c}{\partial x} + \frac{\partial}{\partial y} D \frac{\partial c}{\partial y} + \frac{\partial}{\partial z} D \frac{\partial c}{\partial z} \tag{1.1}$$

$$D\partial_z c\big|_{z=+h/2} = -\frac{\partial a_+(x,y)}{\partial t} = k_{de} a_+ - k_{ad} c\Big|_{z=+h/2}$$

$$D\partial_z c\big|_{z=-h/2} = -\frac{\partial a_-(x,y)}{\partial t} = k_{de} a_- - k_{ad} c\Big|_{z=-h/2}$$

The boundary conditions describe the absorption and desorption of the products from the walls of the channel, placed at $z = h/2$ and $z = -h/2$.
An equation for the variation of the product concentration averaged in the z direction, $\bar{c}$, over time follows directly from Equation (1.1), and has the form:

$$\frac{\partial \bar{c}}{\partial t} = -\frac{\partial \bar{v}_x \bar{c}}{\partial x} - \frac{\partial \bar{v}_y \bar{c}}{\partial y} + \frac{\partial}{\partial x}\bar{D}\frac{\partial \bar{c}}{\partial x} + \frac{\partial}{\partial y}\bar{D}\frac{\partial \bar{c}}{\partial y} - \frac{\partial J_x}{\partial x} - \frac{\partial J_y}{\partial y} - \frac{2}{h}\frac{\partial a}{\partial t} \tag{1.2}$$

where, $\bar{c}$ and $\bar{D}$ are the average values of the concentration and diffusion coefficient in the z direction.

J_x and J_y are defined:

$$J_x \equiv \frac{1}{h}\int_{-h/2}^{h/2}(v_x \delta c - D\frac{\partial \delta c}{\partial x})dz \tag{1.3}$$

$$J_y \equiv \frac{1}{h}\int_{-h/2}^{h/2}(v_y \delta c - D\frac{\partial \delta c}{\partial y})dz \tag{1.4}$$

We define δc as the deviation from the average concentration, $\bar{c}$. It also follows from Equation (1.1) that:

$$\frac{\partial \delta c}{\partial t} = -\frac{\partial \delta v_x \bar{c}}{\partial x} - \frac{\partial \delta v_y \bar{c}}{\partial y} + \frac{\partial}{\partial z}D\frac{\partial \delta c}{\partial z} + \frac{\partial J_x}{\partial x} + \frac{\partial J_y}{\partial y} + \frac{2}{h}\frac{\partial a}{\partial t} + \frac{\partial}{\partial x}\delta D\frac{\partial \bar{c}}{\partial x} + \frac{\partial}{\partial y}\delta D\frac{\partial \bar{c}}{\partial y} \tag{1.5}$$
$$-\frac{\partial v_x \delta c}{\partial x} - \frac{\partial v_y \delta c}{\partial y} + \frac{\partial}{\partial x}D\frac{\partial \delta c}{\partial x} + \frac{\partial}{\partial y}D\frac{\partial \delta c}{\partial y}$$

$$D\frac{\partial \delta c}{\partial z}\bigg|_{z=\pm h/2} = \mp\frac{\partial a_\pm}{\partial t}, \quad \int_{-h/2}^{h/2}\delta c dz = 0, \quad \frac{\partial a_\pm}{\partial t} = -k_{de}a_\pm + k_{ad}c\big|_{z=\pm h/2}$$

where δD is the deviation from the average diffusion coefficient, $\bar{D}$. As discussed by Taylor[1] and Aris[2], we will assume that variation of concentration with depth, δc, is small but the partial derivative of concentration with depth, $\frac{\partial c}{\partial z}$ is significant. It follows that $\frac{\partial c}{\partial t} = \frac{\partial \delta c}{\partial t} \simeq 0$, $\frac{\partial J_x}{\partial x} \simeq 0$, and $\frac{\partial J_y}{\partial y} \simeq 0$ and also the last four terms of Equation (1.5) are negligible. Nevertheless, the values of $\frac{\partial J_x}{\partial x}$ and $\frac{\partial J_y}{\partial y}$ are not negligible in Equation (1.2). According to Gill and Sankarasubramanian,[4] these terms in Equation (1.2), as shown in expression (1.11), are proportional to h, but if we take them into account in Equation (1.5), then the changes of $\frac{\partial J_x}{\partial x}$ and $\frac{\partial J_y}{\partial y}$ in Equation (1.2) will be proportional to h^2. For finding the average concentration (in the z direction), we used concentration deconvolutions by powers of h, limited to the first order only.

Based on these assumptions, the equation for the third term of Equation (1.5), which deals with the variation of diffusion with z, can be simplified to:

$$\frac{\partial}{\partial z}D\frac{\partial \delta c}{\partial z} \approx \frac{\partial}{\partial x}(\delta v_x - \delta D\frac{\partial}{\partial x})\bar{c} + \frac{\partial}{\partial y}(\delta v_y - \delta D\frac{\partial}{\partial y})\bar{c} - \frac{2}{h}\frac{\partial a}{\partial t} \tag{1.6}$$

$$\int_{-h/2}^{h/2}\delta c dz = 0, \quad \frac{\partial \delta c}{\partial z}\bigg|_{z=\pm h/2} = \mp\frac{1}{D}\frac{\partial a}{\partial t}, \quad \frac{\partial a}{\partial t} \approx k_{ad}\bar{c} - k_{de}a$$

Using the conditions described in Equation (1.5), it is possible to show that:

$$\frac{\partial J_x}{\partial x}+\frac{\partial J_y}{\partial y}=\frac{-1}{h}\int_{-h/2}^{h/2}\left(\frac{\partial}{\partial x}(\omega_x-\psi\frac{\partial}{\partial x})+\frac{\partial}{\partial y}(\omega_y-\psi\frac{\partial}{\partial y})\right)\frac{\partial\delta c}{\partial z}dz \tag{1.7}$$

where the introduced parameters ω and ψ describe the variation of velocity and diffusion coefficient in the z direction. Their definitions are:

$$\omega_f(z)=\int_{-h/2}^{z}\delta v_f(z')dz' \tag{1.8}$$

The subscript f refers to the x and y directions.

$$\psi=\int_{-h/2}^{z}\delta D(z')dz' \tag{1.9}$$

Adding an arbitrary constant to the expression to be integrated in Equation (1.7), has no effect on the result of integration. This is illustrated in Equation (1.10), using the boundary conditions of Equation (1.6). The solution for the partial derivative with respect to z of the deviation from the average concentration in the z direction is:

$$\frac{\partial\delta c}{\partial z}\approx\frac{1}{D(z)}\left(\frac{\partial}{\partial x}(\omega_x-\psi\frac{\partial}{\partial x})+\frac{\partial}{\partial y}(\omega_y-\psi\frac{\partial}{\partial y})\right)\overline{c}-\frac{2z}{hD(z)}\frac{\partial a}{\partial t} \tag{1.10}$$

Substitution of Equation (1.10) into Equation (1.7) gives:

$$\frac{\partial J_x}{\partial x}+\frac{\partial J_y}{\partial y}=\frac{-1}{h}\int_{-h/2}^{h/2}\left(\frac{\partial}{\partial x}(\omega_x-\psi\frac{\partial}{\partial x})+\frac{\partial}{\partial y}(\omega_y-\psi\frac{\partial}{\partial y})\right)^2\frac{dz}{D(z)}\overline{c} \tag{1.11}$$
$$+\frac{2}{h^2}\int_{-h/2}^{h/2}\left(\frac{\partial}{\partial x}(\omega_x-\psi\frac{\partial}{\partial x})+\frac{\partial}{\partial y}(\omega_y-\psi\frac{\partial}{\partial y})\right)\frac{zdz}{D(z)}\frac{\partial a}{\partial t}$$

Equation (1.11) is the most general form of the equation for average concentration and applies before a steady state is reached, when the surface concentrations of products on the walls of the μFFE device have reached constant values. Once this steady state is reached, $\frac{\partial a}{\partial t}=0$ so that we can eliminate the second integral from Equation (1.11). We will also assume, that the parameters in Equation (1.11) do not depend on the coordinates x and y. Based on these two assumptions, Equation (1.11) can be simplified to:

$$\frac{\partial J_x}{\partial x}+\frac{\partial J_y}{\partial y}=-\sum_{f,g=x,y}\gamma_{fg}\frac{\partial^2\overline{c}}{\partial f\,\partial g}+\Phi\left(\frac{\partial^2}{\partial x^2}+\frac{\partial^2}{\partial y^2}\right)^2\overline{c}+\sum_{f=x,y}\Omega_f\frac{\partial}{\partial f}\left(\frac{\partial^2}{\partial x^2}+\frac{\partial^2}{\partial y^2}\right)\overline{c} \tag{1.12}$$

where the parameters γ, Ω and Φ describe diffusion in the x and y directions, asymmetry and higher moments of the concentration distributions respectively and have definitions:

$$\gamma_{fg}\equiv\int_{-h/2}^{h/2}\frac{\omega_g\omega_f dz}{hD} \tag{1.13}$$

$$\Omega_f\equiv\int_{-h/2}^{h/2}\frac{2\omega_f\psi dz}{hD} \tag{1.14}$$

In both of the equations above, the subscripts f or g refer to the x or y directions.

$$\Phi \equiv \int_{-h/2}^{h/2} \frac{\psi^2 dz}{hD} \tag{1.15}$$

Substitution of Equation (1.12) in Equation (1.2), for the stationary and space-independent case, gives:

$$\left(\overline{v}_x \frac{\partial}{\partial x} + \overline{v}_y \frac{\partial}{\partial y}\right)\overline{c} = \overline{D}\left(\frac{\partial^2}{\partial x^2} + \frac{\partial^2}{\partial y^2}\right)\overline{c} + \sum_{f,g=x,y} \gamma_{fg} \frac{\partial^2}{\partial f \partial g}\overline{c} + \Phi\left(\frac{\partial^2}{\partial x^2} + \frac{\partial^2}{\partial y^2}\right)^2 \overline{c} \tag{1.16}$$
$$- \sum_{f=x,y} \Omega_f \frac{\partial}{\partial f}\left(\frac{\partial^2}{\partial x^2} + \frac{\partial^2}{\partial y^2}\right)\overline{c}$$

2. General expression for peak broadening

The boundary conditions for Equation (1.16) are:

$$\overline{c}(x,0,t) = \begin{cases} 0, |x| > w_0/2 \\ \overline{c}_0, |x| \le w_0/2 \end{cases} \tag{2.1}$$

where w_0 is the width of the product stream as it enters the separation channel. Additionally, we shall assume that there is no average flow in the x direction as there are side walls (see **Figure S-2**). We introduce a new coordinate s, which describes the relative position of the sample at a point in the x-y plane relative to the median of the total product flow.

$$s = x - y\overline{v}_x / \overline{v}_y \tag{2.2}$$

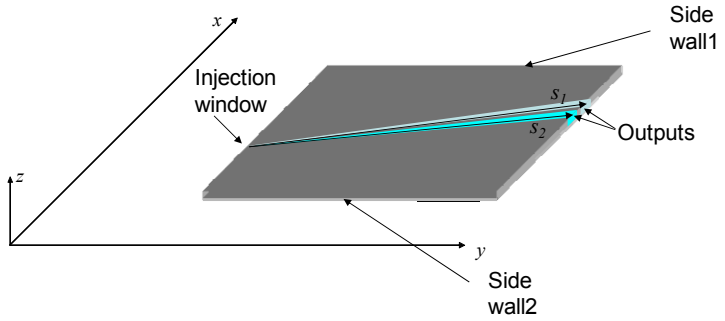

Figure S-2: Illustration of s coordinate systems for two species

We can rewrite Equation (1.16) and the boundary conditions for Equation (2.1) in the form:

$$\overline{v}_y \frac{\partial}{\partial y}\overline{c} = \left(\overline{D} + \gamma_{xx}\right)\frac{\partial^2}{\partial s^2}\overline{c} + 2\gamma_{yx}\hat{\mathrm{L}}\frac{\partial}{\partial s}\overline{c} + \left(\overline{D} + \gamma_{yy}\right)\hat{\mathrm{L}}^2\overline{c} \tag{2.3}$$
$$+ \Phi\left(\frac{\partial^2}{\partial s^2} + \hat{\mathrm{L}}^2\right)^2 \overline{c} - \left(\Omega_x \frac{\partial}{\partial s} + \Omega_y \hat{\mathrm{L}}\right)\left(\frac{\partial^2}{\partial s^2} + \hat{\mathrm{L}}^2\right)\overline{c}$$

$$\overline{c}(s,0,t) = \begin{cases} 0, |s| > w_0/2 \\ \overline{c}_0, |s| \le w_0/2 \end{cases}$$

where the operator, $\hat{\mathrm{L}}$ has the definition:

$$\hat{\mathrm{L}} = \frac{\partial}{\partial y} - \frac{\overline{v}_x}{\overline{v}_y}\frac{\partial}{\partial s} \tag{2.4}$$

New coordinates (y, s) are a result of defining a non-orthogonal transformation of initial coordinates (y, x). In the (y, s) coordinates, y represents the direction of the hydrodynamic flow while s represents the median direction of a stream of a deflected species. Derivatives with respect to y are much smaller than derivatives with respect to s. By assuming, that the partial derivative with respect to y in $\hat{\mathrm{L}}$ is negligible, we can simplify the expression for the operator in Equation (2.4):

$$\hat{\mathrm{L}} \approx -\frac{\overline{v}_x}{\overline{v}_y}\frac{\partial}{\partial s} \tag{2.5}$$

Equation (2.3) will take the form:

$$\overline{v}_y \frac{\partial}{\partial y}\overline{c} = \left(\overline{D} + \gamma_{xx} - 2\gamma_{yx}\frac{\overline{v}_x}{\overline{v}_y} + \left(\overline{D} + \gamma_{yy}\right)\left(\frac{\overline{v}_x}{\overline{v}_y}\right)^2 \right)\frac{\partial^2}{\partial s^2}\overline{c} + \Phi\left(1 + \left(\frac{\overline{v}_x}{\overline{v}_y}\right)^2\right)^2 \frac{\partial^4}{\partial s^4}\overline{c} \tag{2.6}$$

$$-\left(\Omega_x - \Omega_y\frac{\overline{v}_x}{\overline{v}_y}\right)\left(1 + \left(\frac{\overline{v}_x}{\overline{v}_y}\right)^2\right)\frac{\partial^3}{\partial s^3}\overline{c}$$

Based on Equation (2.6), we can find expressions for the moments, M_n, as functions of y, defined as:

$$\mathrm{M}_n(y) \equiv \int_{-\infty}^{\infty} \overline{c}(s,y)s^n ds \tag{2.7}$$

The zero moment M_0 reflects the total flow of the products to be separated, the first moment divided by the zero moment (M_1/ M_0) describes the median of the distribution as a function of s, the second moment (M_2 / M_0) reflects the variance of the distribution σ^2_x, and so on. Equations for the moments have the form:

$$\frac{\partial \mathrm{M}_n}{\partial y / \overline{v}_y} = n(n-1)\left(\overline{D} + \gamma_{xx} - 2\gamma_{yx}\frac{\overline{v}_x}{\overline{v}_y} + \left(\overline{D} + \gamma_{yy}\right)\left(\frac{\overline{v}_x}{\overline{v}_y}\right)^2 \right)\mathrm{M}_{n-2} \tag{2.8}$$

$$+\left(\frac{\overline{v}_x}{\overline{v}_y}\Omega_y - \Omega_x\right)\left(1 + \left(\frac{\overline{v}_x}{\overline{v}_y}\right)^2\right) n(n-1)(n-2)\mathrm{M}_{n-3} +$$

$$+\left(1 + \left(\frac{\overline{v}_x}{\overline{v}_y}\right)^2\right)^2 n(n-1)(n-2)(n-3)\mathrm{M}_{n-4}$$

where it is assumed, that M_n is zero for negative values of n.
According to the boundary conditions for Equation (2.3), at $y = 0$, the first three moments have the values:

$$\mathrm{M}_0(0) = w_0\overline{c}_0, \quad \mathrm{M}_1(0) / \mathrm{M}_0(0) = 0, \quad \mathrm{M}_2(0) / \mathrm{M}_0(0) = w_0^{\,2} / 12 \tag{2.9}$$

Only M_2 changes for $y > 0$:

$$\sigma_x^2 = \mathrm{M}_2(t)/\mathrm{M}_0(t) = {w_0}^2/12 + \frac{2y}{\overline{v}_y}\left(\gamma_{xx} - 2\gamma_{yx}\frac{\overline{v}_x}{\overline{v}_y} + \gamma_{yy}\left(\frac{\overline{v}_x}{\overline{v}_y}\right)^2 + \overline{D}\left(1+\left(\frac{\overline{v}_x}{\overline{v}_y}\right)^2\right)\right) \tag{2.10}$$

According to Equation (2.10), we need to calculate an expression for the dispersion, Θ:

$$\Theta = \gamma_{xx} - 2\gamma_{yx}\frac{\overline{v}_x}{\overline{v}_y} + \gamma_{yy}\left(\frac{\overline{v}_x}{\overline{v}_y}\right)^2 \tag{2.11}$$

$$= \int_{-h/2}^{h/2}\left(\omega_x - \omega_y\frac{\overline{v}_x}{\overline{v}_y}\right)^2\frac{dz}{hD}$$

$$= \int_{-h/2}^{h/2}\left(\int_{-h/2}^{z}\left(\delta v_x(z') - \frac{\overline{v}_x}{\overline{v}_y}\delta v_y(z')\right)dz'\right)^2\frac{dz}{hD}$$

If the distance to the collector in the y direction is L, than in Equation (2.10), $y = L$.

3. Determination of the velocity profiles

In their most general forms, equations for velocity profiles should include the influence of temperature on viscosity, diffusion and electrophoretic mobility that results from Joule heating effects. To describe the temperature profile within the separation channel, we use the well-known expression: [5]

$$\Delta T(z) = \frac{\kappa E^2\left(h^2 - 4z^2\right)}{8\lambda} \tag{3.1}$$

In Equation (3.1), we assume that the electrical conductivity, κ, the thermal conductivity λ and the power density of the electric field, proportional to E^2, do not depend on the coordinates. Actually, these dependencies do exist, but we will assume, that they are insignificant, provided that the temperature difference between the walls and the electrolyte at $z = 0$, ΔT ($z = 0$) << T_0, the temperature of the walls. We also assume that the electric field is a constant.

For the relatively small temperature changes in μFFE, we assume a linear dependence of dynamic viscosity, η, with temperature:

$$\eta(T) = \eta(T_0)\left[1 + \alpha_\eta \Delta T\right] \tag{3.2}$$

where $\alpha_\eta = -2.28 \times 10^{-2}$ K^{-1} at SLC, is the temperature coefficient of dynamic viscosity for aqueous electrolytes.

For electrophoretic flow combined with hydrodynamic flow initiated by pressure, the total velocity of the product streams is the superposition of two independent parts, one is proportional to the electric field strength, and the other is proportional to the pressure gradient.

$$v(z) = v_{\mathrm{hd}}(z) + \mu_{\mathrm{ep}}(z)E + v_{\mathrm{EOF}} = v_{\mathrm{hd}}(z) + \left\{\mu_{\mathrm{ep}}(z) + \mu_{\mathrm{EOF}}\right\}E \tag{3.3}$$

The electroosmotic mobility is independent of the temperature in the middle of the flow ($z = 0$) but depends on the electrical permittivity, ε, zeta-potential, ζ, and viscosity at the edge of the Stern layer, a few nanometres from the wall.

$$\mu_{\mathrm{EOF}} = \frac{v_{\mathrm{EOF}}}{E} = -\frac{\varepsilon\varsigma}{\eta} \tag{3.4}$$

As the electroosmotic mobility only varies with the z coordinate in the thin electrical double layer near the walls, and the thickness of the double layer is negligible compared to the depth of the channel,[6] we do not take into account variations of the electroosmotic velocity with z. We assume that the electroosmotic mobility in Equation (3.4) only depends on the physical properties of the electrolyte near the wall. As E_z = 0, we only write expressions for the electroosmotic velocity in the x and y directions; there is no electroosmotic velocity in the z direction.

$$v_{\mathrm{EOF},x} = \mu_{\mathrm{EOF}}(T_0)E_x, \quad v_{\mathrm{EOF},y} = \mu_{\mathrm{EOF}}(T_0)E_y, \text{ and } \quad v_{\mathrm{EOF},z} = 0 \tag{3.5}$$

Equation (3.6) gives a definition for electrophoretic mobility

$$\mu_{\mathrm{ep}} = \frac{v_{\mathrm{ep}}}{E} = \frac{q}{6\pi\eta r_{\mathrm{h}}} \tag{3.6}$$

where q is the charge on the product molecule and r_{h} is its hydrodynamic radius. For small increases in temperature, electrophoretic mobility increases linearly with temperature due to its reciprocal dependence on viscosity.[7]

$$\mu_{\mathrm{ep}}(T) = \mu_{\mathrm{ep}}(T_0)\left[1 + \alpha_{\mu}\Delta T\right] \tag{3.7}$$

In Equation (3.7), α_{μ} is the temperature coefficient for electrophoretic mobility. Electrophoretic mobility is depth dependent, due to the temperature induced variation of viscosity with depth.

$$v_{\mathrm{ep},x} = \mu_{\mathrm{ep}}(T_0, z)E_x, \quad v_{\mathrm{ep},y} = \mu_{\mathrm{ep}}(T_0, z)E_y, \quad v_{\mathrm{ep},z} = 0 \tag{3.8}$$

By combining Equations (3.1) and (3.7), we obtain an equation for the electrophoretic mobility as a function of z.

$$\mu_{\mathrm{ep}}(z) = \mu_{\mathrm{ep}}(T_0)\left[1 + \frac{\alpha_{\mu}\kappa E^2\left(h^2 - 4z^2\right)}{8\lambda}\right] \tag{3.9}$$

If we assume that hydrodynamic flow depends only on the z coordinate, we can write a definitive expression for hydrodynamic flow:

$$\frac{\partial}{\partial z}\eta(z)\frac{\partial}{\partial z}v_{\mathrm{hd},g}(z) = -\frac{\partial}{\partial g}p(x,y), \quad g = x, y \tag{3.10}$$

where p is the pressure. Equation (3.10) can only be satisfied if pressure depends linearly on the coordinates x and y, and their corresponding derivatives are constants. In this case, the general solution to Equation (3.10) is symmetrical about the plane z=0 and has the form:

$$v_{\mathrm{hd},g}(z) = -\int_0^z \frac{z'dz'}{\eta(z')}\frac{\partial}{\partial g}p(x,y) + \tilde{v}_{\mathrm{hd},g}, \quad g = x, y \tag{3.11}$$

where the values of $v_{\mathrm{hd},g}$ are independent of the x,y-coordinates, and can be defined by the boundary conditions and $\tilde{v}_{\mathrm{hd},g}$ is a constant of integration.

The are different boundary conditions in the x and y directions. In the x direction, flow is restricted by the presence of the side walls so that there is zero total flow (see **Figure S-2**). The boundary condition can be written as:

$$v_{\mathrm{hd},x}\left(z = \pm\frac{h}{2}\right) = 0, \quad \int_{-h/2}^{h/2}\left(v_{\mathrm{hd},x}(z) + v_{\mathrm{EOF},x}\right)dz = 0 \tag{3.12}$$

In the *y* direction, there is free hydrodynamic flow determined by the pressure gradient with zero flow at the upper and lower walls:

$$v_{\mathrm{hd},g}(z=\pm\frac{h}{2})=0 \tag{3.13}$$

It follows that the boundary conditions that apply to hydrodynamic flow in μFFE are:

$$v_{\mathrm{hd},x}(z=\pm\frac{h}{2})=0,\quad \int_{-h/2}^{h/2}\left(v_{\mathrm{hd},x}(z)+v_{\mathrm{EOF},x}\right)dz=0,\quad v_{\mathrm{hd},y}(z=\pm\frac{h}{2})=0 \tag{3.14}$$

Combining Equations (3.5), (3.11) and (3.14), and taking into account the symmetry about the plane z=0, we can obtain expressions for the total velocity of the electrolyte in the *x* and *y* directions:

$$v_{\mathrm{buf},x}(z)=\mu_{\mathrm{EOF}}(T_0)E_x-\int_{-h/2}^{z}\frac{z'dz'}{\eta(z')}\frac{\partial p}{\partial x},\qquad \int_{-h/2}^{h/2}v_{\mathrm{buf},x}(z)dz=0 \tag{3.15}$$

$$v_{\mathrm{buf},y}(z)=\mu_{\mathrm{EOF}}(T_0)E_y-\int_{-h/2}^{z}\frac{z'dz'}{\eta(z')}\frac{\partial p}{\partial y} \tag{3.16}$$

where v_{buf} is the total velocity of the electrolyte resulting from electroosmotic and hydrodynamic flow. For the derivative of pressure with respect to *x* in Equation (3.15), we find:

$$\frac{\partial p}{\partial x}=-h\mu_{\mathrm{EOF}}(T_0)E_x\Big/\int_{-h/2}^{h/2}\frac{z^2dz}{\eta(z)} \tag{3.17}$$

And finally, for the velocity profile in the *x* direction:

$$v_{\mathrm{buf},x}(z)=\mu_{\mathrm{EOF}}(T_0)E_x\left(1+h\int_{-h/2}^{z}\frac{z'dz'}{\eta(z')}\Big/\int_{-h/2}^{h/2}\frac{z^2dz}{\eta(z)}\right) \tag{3.18}$$

Combining Equations (3.1) and (3.2), and assuming that variation of temperature in the *z* direction is relatively small, we obtain the approximation:

$$\frac{1}{\eta(T)}\approx\frac{1-\alpha_\eta\Delta T}{\eta(T_0)}=\frac{1}{\eta(T_0)}-\frac{\alpha_\eta\kappa E^2\left(h^2-4z^2\right)}{8\lambda\eta(T_0)} \tag{3.19}$$

Using Equations (3.16), (3.18) and (3.19), we can derive expressions for the velocity profiles in the *x* and *y* directions:

$$v_{\text{buf},x}(z) \approx \mu_{\text{EOF}}(T_0)E_x\left(1+\frac{h\int_{-h/2}^{z}\left(1-\frac{\alpha_\eta\kappa E^2\left(h^2-4z'^2\right)}{8\lambda}\right)z'dz'}{\int_{-h/2}^{h/2}\left(1-\frac{\alpha_\eta\kappa E^2\left(h^2-4z'^2\right)}{8\lambda}\right)z'^2\,dz'}\right) \tag{3.20}$$

$$= \mu_{\text{EOF}}(T_0)E_x\left(1+\int_{1}^{(2z/h)}\left(1-\Lambda\left(1-\theta^2\right)\right)d\theta^2 \Big/ \int_{-1}^{1}\left(1-\Lambda\left(1-\theta^2\right)\right)\theta^2 d\theta\right)$$

where dimensionless Λ is the maximum fractional change to viscosity as a result temperature differences:

$$\Lambda=\frac{\alpha_\eta\kappa E^2h^2}{8\lambda} \tag{3.21}$$

and θ is the dimensionless position in the z direction.

$$\theta=\frac{2z}{h} \tag{3.22}$$

In the y direction, the expression for the velocity profile is:

$$v_{\text{buf},y}(z) \approx \mu_{\text{EOF}}(T_0)E_y - \int_{-h/2}^{z}\left(1-\frac{\alpha_\eta\kappa E^2\left(h^2-4z'^2\right)}{8\lambda}\right)\frac{z'dz'}{\eta(T_0)}\frac{\partial p}{\partial y} \tag{3.23}$$

$$= \mu_{\text{EOF}}(T_0)E_y - \Upsilon\int_{1}^{(2z/h)}\left(1-\Lambda\left(1-\theta^2\right)\right)d\theta^2$$

where Υ is the hydrodynamic velocity at ($z = 0$) if $T = T_0$.

$$\Upsilon=\frac{h^2}{8\eta(T_0)}\frac{\partial p}{\partial y} \tag{3.24}$$

By evaluating the integrals in Equations (3.20) and (3.23), we reach the final expressions:

$$v_{\text{buf},x}(z) \approx \mu_{\text{EOF}}(T_0)E_x\left(1+\frac{\left((2z/h)^2-1\right)\left(1+\frac{\Lambda}{2}\left((2z/h)^2-1\right)\right)}{2/3-4\Lambda/15}\right) \tag{3.25}$$

$$v_{\text{buf},y}(z) \approx \mu_{\text{EOF}}(T_0)E_y - \left((2z/h)^2-1\right)\left(1+\frac{\Lambda}{2}\left((2z/h)^2-1\right)\right)\Upsilon \tag{3.26}$$

The average values for the electrolyte velocities in the x and y directions are:

$$\overline{v}_{\text{buf},x} = 0 \tag{3.27}$$

$$\overline{v}_{\text{buf},y} \approx \mu_{\text{EOF}}(T_0)E_y + \left(\frac{2}{3}-\frac{4}{15}\Lambda\right)\Upsilon \tag{3.28}$$

As observed in macro-FFE devices,[3] there is recirculation of the electroosmotic flow in the *x*-*z* plane. At the top and bottom walls ($z = \pm h/2$), there is EOF in the absence of pressure, but when the flow reaches the side walls, it moves up or down to $z = 0$ before travelling along the *x* axis as a reversed flow such that:

$$v_{\mathrm{EOF}}\left(z = 0\right) \approx -\tfrac{1}{2} v_{\mathrm{EOF}}(z = \pm h/2) \tag{3.29}$$

And for the variations of the velocities (from the average values):

$$\delta v_{\mathrm{buf},x}(z) \approx \frac{15\mu_{\mathrm{EOF}}(T_0)E_x}{10-4\Lambda}\left(\frac{\Lambda}{2}\left(\left(\frac{2z}{h}\right)^4 - 2\left(\frac{2z}{h}\right)^2 + \frac{7}{15}\right) + \left(\frac{2z}{h}\right)^2 - \frac{1}{3}\right) \tag{3.30}$$

$$\delta v_{\mathrm{buf},y}(z) \approx -\Upsilon\left(\frac{\Lambda}{2}\left(\left(\frac{2z}{h}\right)^4 - 2\left(\frac{2z}{h}\right)^2 + \frac{7}{15}\right) + \left(\frac{2z}{h}\right)^2 - \frac{1}{3}\right) \tag{3.31}$$

Equations for electrophoretic velocities will be of the form:

$$v_{\mathrm{ep},g} = \mu_{\mathrm{ep}}(T_0)E_g\left(1 + P\left(1-(2z/h)^2\right)\right), g = x, y \tag{3.32}$$

where *P* is dimensionless and equals the maximum fractional change in electrophoretic mobility as a result of temperature differences between the electrolyte at the centre of the channel and near the walls.

$$P = \frac{\alpha_{\mu}\kappa E^2 h^2}{8\lambda} \tag{3.33}$$

For the average electrophoretic velocity and deviation from the average electrophoretic velocity, we have:

$$\overline{v}_{\mathrm{ep},g} = \mu_{\mathrm{ep}}(T_0)E_g\left(1 + 2P/3\right) \tag{3.34}$$

$$\delta v_{\mathrm{ep},g} = \mu_{\mathrm{ep}}(T_0)E_g P\left(1/3 - (2z/h)^2\right) \tag{3.35}$$

The average total velocities of the product streams are the sums of their average electrophoretic velocities and the average buffer velocities (see Equation (3.27) and (3.28)):

$$\overline{v}_x = \mu_{\mathrm{ep}}(T_0)E_x\left(1 + 2P/3\right) \tag{3.36}$$

$$\overline{v}_y \approx \mu_{\mathrm{EOF}}(T_0)E_y + \left(\frac{2}{3} - \frac{4}{15}\Lambda\right)\Upsilon + \mu_{\mathrm{ep}}(T_0)E_y\left(1 + 2P/3\right) \tag{3.37}$$

In Equation (2.11), we consider the linear combination of their deviations from the mean velocity rather than analysing the deviations in the *x* and *y* direction separately. Taking into account Equations (3.30) and (3.34), Equation (2.11) can be simplified to:

$$\delta v_x - \frac{\overline{v}_x}{\overline{v}_y}\delta v_y = \chi_0 + \chi_1\left(\frac{2z}{h}\right)^2 - 5\left(\chi_0 + \frac{1}{3}\chi_1\right)\left(\frac{2z}{h}\right)^4 \tag{3.38}$$

where χ_0 and χ_1 and are parameters that can be used to simplify the expression (3.38):

$$\chi_0 = \frac{\mu_{\mathrm{ep}}P}{3}\left(E_x - \frac{\overline{v}_x}{\overline{v}_y}E_y\right) + \left(\frac{15\mu_{\mathrm{EOF}}E_x}{10-4\Lambda} + \frac{\overline{v}_x}{\overline{v}_y}\Upsilon\right)\left(\frac{7\Lambda}{30} - \frac{1}{3}\right) \tag{3.39}$$

$$\chi_1 = -3\chi_0 - \frac{3\Lambda}{10}\left(\frac{15\mu_{\mathrm{EOF}}E_x}{10-4\Lambda} + \frac{\overline{v}_x}{\overline{v}_y}\Upsilon\right) \tag{3.40}$$

Now that we have equations for the velocity profiles in the *x* and y directions, we can substitute these into the equation for dispersion to find the total variance.

II. Derivation of a general equation for resolution, R_S

Equation (2.11) can be rewritten as:

$$\Theta = \frac{h^2}{8}\int_{-1}^{1}\left(\int_{-1}^{\theta'}\left(\chi_0 + \chi_1\theta^2 - 5\left(\chi_0 + \frac{1}{3}\chi_1\right)\theta^4\right)d\theta\right)^2 \frac{d\theta'}{D(h\theta'/2)} \tag{4.1}$$

$$= \frac{h^2}{4}\int_{0}^{1}\left(\chi_0\theta + \frac{\chi_1}{3}\theta^3 - 5\left(\chi_0 + \frac{1}{3}\chi_1\right)\theta^5\right)^2 \frac{d\theta}{D(h\theta/2)}$$

For the temperature dependence of the diffusion coefficient, we can use an equation similar to Equation (3.19):

$$\frac{1}{D(z)} \approx \frac{1-\alpha_D\Delta T}{D(T_0)} = \frac{1}{D(T_0)}\left(1-\Gamma\left(1-\left(2z/h\right)^2\right)\right) \tag{4.2}$$

where α_D is the temperature coefficient for the diffusion constant and dimensionless Γ is the fractional increase in the diffusion coefficient as a result of temperature differences.

$$\Gamma = \frac{\alpha_D \kappa E^2 h^2}{8\lambda} \tag{4.3}$$

This allows Equation (4.1) to be presented as:

$$\Theta = \frac{h^2}{4D(T_0)}\int_{0}^{1}\left(\chi_0 + \left(\chi_0 + \frac{\chi_1}{3}\right)\theta^2\right)^2 (1-\theta^2)^2\left(1-\Gamma(1-\theta^2)\right)\theta^2 d\theta \tag{4.4}$$

$$= \frac{2h^2}{D(T_0)}\left(\begin{array}{l}\dfrac{{\chi_0}^2}{3\times5\times7}\left(1-\dfrac{2\Gamma}{3}\right) + \dfrac{2\chi_0\left(\chi_0+\chi_1/3\right)}{5\times7\times9}\left(1-\dfrac{6\Gamma}{11}\right) + \\ + \dfrac{\left(\chi_0+\chi_1/3\right)^2}{7\times9\times11}\left(1-\dfrac{8\Gamma}{13}\right)\end{array}\right)$$

We suggested earlier, temperature differences between the electrolyte at $z = 0$ and at the walls are small. It follows that the parameters Λ, P and Γ are also small. Accordingly the parameters in Equation (3.38) can be simplified:

$$\frac{\chi_1}{3} + \chi_0 \approx -\frac{\Lambda}{10}\left(\frac{3\mu_{EOF}E_x}{2} + \frac{\overline{v}_x}{\overline{v}_y}\Upsilon\right) \tag{4.5}$$

$$\chi_0 \approx \frac{\mu_{ep}P}{3}\left(E_x - \frac{\overline{v}_x}{\overline{v}_y}E_y\right) - \left(\frac{\mu_{EOF}E_x}{2} + \frac{\overline{v}_x}{3\overline{v}_y}\Upsilon\right) + \frac{\Lambda}{10}\left(\frac{3\mu_{EOF}E_x}{2} + \frac{7}{3}\frac{\overline{v}_x}{\overline{v}_y}\Upsilon\right)$$

Using the same reasoning, the equation for dispersion can also be simplified. Thus Equation (4.4) simplifies to:

$$\Theta \approx \frac{2h^2}{105D(T_0)}\left(\frac{\mu_{\mathrm{EOF}}E_x}{2}+\frac{\overline{v}_x}{3\overline{v}_y}\Upsilon\right)\left(\begin{array}{l}\left(\frac{\mu_{\mathrm{EOF}}E_x}{2}+\frac{\overline{v}_x}{3\overline{v}_y}\Upsilon\right)-\mu_{\mathrm{ep}}P\left(E_x-\frac{\overline{v}_x}{\overline{v}_y}E_y\right)\\ -\left(\frac{\Lambda}{5}+\frac{\Gamma}{3}\right)\mu_{\mathrm{EOF}}E_x-\left(\frac{\Lambda}{5}+\frac{\Gamma}{9}\right)\frac{2\overline{v}_x}{\overline{v}_y}\Upsilon\end{array}\right) \tag{4.6}$$

For the small increases in temperature associated with μFFE, the contribution to dispersion from variations in electrophoretic mobility, viscosity, and diffusion coefficients are negligible; so to a good approximation, Equation (4.6) can be further simplified to:

$$\Theta \approx \frac{2h^2}{105D(T_0)}\left(\frac{\mu_{\mathrm{EOF}}E_x}{2}+\frac{\overline{v}_x}{3\overline{v}_y}\Upsilon\right)^2 \tag{4.7}$$

Using Equation (3.28) we can write the parameter, Υ as function of the average hydrodynamic velocity:

$$\Upsilon \approx \frac{3}{2\left(1-2\Lambda/5\right)}\overline{v}_{\mathrm{hd}} \tag{4.8}$$

Using Equation (4.8), Equation (4.6) can be approximately rewritten in the form:

$$\Theta \approx \frac{h^2}{105D(T_0)}\left(\mu_{\mathrm{EOF}}E_x+\frac{\overline{v}_x}{\overline{v}_y}\overline{v}_{\mathrm{hd}}\right)\times \left(\left(\mu_{\mathrm{EOF}}E_x+\frac{\overline{v}_x}{\overline{v}_y}\overline{v}_{\mathrm{hd}}\right)\left(\frac{1}{2}-\left(\frac{\Lambda}{5}+\frac{\Gamma}{3}\right)\right)-\mu_{\mathrm{ep}}P\left(E_x-\frac{\overline{v}_x}{\overline{v}_y}E_y\right)\right) \tag{4.9}$$

If we assume that heating effects are negligible, combining (4.7) and(4.8), we obtain:

$$\Theta \approx \frac{h^2}{210D(T_0)}\left(\mu_{\mathrm{EOF}}E_x+\frac{\overline{v}_x}{\overline{v}_y}\overline{v}_{\mathrm{hd}}\right)^2 \tag{4.10}$$

If we assume that heating effects are negligible, from Equation (2.10) we can show:

$$\sigma_x = \sqrt{\frac{{w_0}^2}{12}+\frac{2L}{\overline{v}_y}\left(\frac{h^2}{210D}\left(\mu_{\mathrm{EOF}}E_x+\frac{\overline{v}_x}{\overline{v}_y}\overline{v}_{\mathrm{hd}}\right)^2+D\left(1+\left(\frac{\overline{v}_x}{\overline{v}_y}\right)^2\right)\right)} \tag{4.11}$$

The average *x* coordinate of a stream as it exits the separation channel is:

$$\overline{x} = \frac{\overline{v}_x}{\overline{v}_y}L \tag{4.12}$$

If we have two species, with differing electrophoretic mobilities, μ_{ep1} and μ_{ep2}, then their difference in position at the *x* axis will be approximately:

$$\Delta\overline{x} = \left|\frac{\overline{v}_{x,1}}{\overline{v}_{y,1}}-\frac{\overline{v}_{x,2}}{\overline{v}_{y,2}}\right|L \tag{4.13}$$

As a criterion of resolution, R_S, the quotient of $\Delta\overline{x}$ to the average peak width, $w = 4\sigma_x$, can be used:[7]

$$R_{\mathrm{S}} = \frac{\Delta \overline{x}}{2\left(\sigma_{1,x} + \sigma_{2,x}\right)} \tag{4.14}$$

Where, according to Equation (4.11) expressions for variance of the products streams are:

$$\sigma_{1,x} = \sqrt{\frac{{w_0}^2}{12} + \frac{2L}{\overline{v}_{1,y}}\left(\frac{h^2}{210D_1}\left(\mu_{\mathrm{EOF}}E_x + \frac{\overline{v}_{1,x}}{\overline{v}_{1,y}}\overline{v}_{\mathrm{hd}}\right)^2 + D_1\left(1 + \left(\frac{\overline{v}_{1,x}}{\overline{v}_{1,y}}\right)^2\right)\right)} \tag{4.15}$$

$$\sigma_{2,x} = \sqrt{\frac{{w_0}^2}{12} + \frac{2L}{\overline{v}_{2,y}}\left(\frac{h^2}{210D_2}\left(\mu_{\mathrm{EOF}}E_x + \frac{\overline{v}_{2,x}}{\overline{v}_{2,y}}\overline{v}_{\mathrm{hd}}\right)^2 + D_2\left(1 + \left(\frac{\overline{v}_{2,x}}{\overline{v}_{2,y}}\right)^2\right)\right)} \tag{4.16}$$

If heating effects are negligible, equations for average velocities in the *x* and *y* directions are:

$$\overline{v}_x = \mu_{\mathrm{ep}}E_x = \mu_{\mathrm{ep}}E\sin\varphi \tag{4.17}$$

$$\overline{v}_y \approx \left(\mu_{\mathrm{EOF}} + \mu_{\mathrm{ep}}\right)E_y + \overline{v}_{\mathrm{hd}} = \left(\mu_{\mathrm{EOF}} + \mu_{\mathrm{ep}}\right)E\cos\phi + \overline{v}_{\mathrm{hd}} \tag{4.18}$$

By combining equations (4.13), (4.14), (4.15), (4.16), (4.17), and (4.18) we obtain an equation for resolution in the absence of significant Joule heating:

$$R_S = \frac{\left|\frac{\left(\mu_{\mathrm{ep1}} - \mu_{\mathrm{ep2}}\right)LE\sin\varphi\left(\mu_{\mathrm{EOF}}E\cos\varphi + \overline{v}_{\mathrm{hd}}\right)}{\left\{\left(\mu_{\mathrm{EOF}} + \mu_{\mathrm{ep1}}\right)E\cos\varphi + \overline{v}_{\mathrm{hd}}\right\}\left\{\left(\mu_{\mathrm{EOF}} + \mu_{\mathrm{ep2}}\right)E\cos\varphi + \overline{v}_{\mathrm{hd}}\right\}}\right|}{2\left(\sqrt{\frac{{w_0}^2}{12} + \frac{2L}{\left(\mu_{\mathrm{EOF}} + \mu_{\mathrm{ep1}}\right)E\cos\varphi + \overline{v}_{\mathrm{hd}}}\left(\frac{h^2}{210D_1}\left(\mu_{\mathrm{EOF}} + \frac{\mu_{\mathrm{ep1}}\overline{v}_{\mathrm{hd}}}{\left(\mu_{\mathrm{EOF}} + \mu_{\mathrm{ep1}}\right)E\cos\varphi + \overline{v}_{\mathrm{hd}}}\right)^2 E^2\sin^2\varphi + D_1\left(1 + \left(\frac{\mu_{\mathrm{ep1}}E\sin\varphi}{\left(\mu_{\mathrm{EOF}} + \mu_{\mathrm{ep1}}\right)E\cos\varphi + \overline{v}_{\mathrm{hd}}}\right)^2\right)\right)}} + \sqrt{\frac{{w_0}^2}{12} + \frac{2L}{\left(\mu_{\mathrm{EOF}} + \mu_{\mathrm{ep2}}\right)E\cos\varphi + \overline{v}_{\mathrm{hd}}}\left(\frac{h^2}{210D_2}\left(\mu_{\mathrm{EOF}} + \frac{\mu_{\mathrm{ep2}}\overline{v}_{\mathrm{hd}}}{\left(\mu_{\mathrm{EOF}} + \mu_{\mathrm{ep2}}\right)E\cos\varphi + \overline{v}_{\mathrm{hd}}}\right)^2 E^2\sin^2\varphi + D_2\left(1 + \left(\frac{\mu_{\mathrm{ep2}}E\sin\varphi}{\left(\mu_{\mathrm{EOF}} + \mu_{\mathrm{ep2}}\right)E\cos\varphi + \overline{v}_{\mathrm{hd}}}\right)^2\right)\right)}}\right)} \tag{4.19}$$

For band broadening for which the temperature change within the channel is small but significant due to Joule heating, we obtain the more general equation that takes into account changes to viscosity, diffusion coefficients and electrophoretic mobility associated with Joule heating induced temperature differences. Based on Equation (4.9), Equation (4.19) has the more general form:

$$R_S = \frac{\left| \frac{\left(\mu_{ep1} - \mu_{ep2}\right) LE \sin\varphi \left(\mu_{EOF} E\cos\varphi + \overline{v}_{hd}\right)}{\left\{\left(\mu_{EOF} + \mu_{ep1}\right) E\cos\varphi + \overline{v}_{hd}\right\}\left\{\left(\mu_{EOF} + \mu_{ep2}\right) E\cos\varphi + \overline{v}_{hd}\right\}} \right|}{2\left(\sqrt{\frac{w_0^{\,2}}{12} + \frac{2L}{\left(\mu_{EOF} + \mu_{ep1}\right) E\cos\varphi + \overline{v}_{hd}} \left(\begin{array}{l} \frac{h^2 E^2 \sin^2\varphi}{105 D_1} \left(\mu_{EOF} + \frac{\mu_{ep1}\overline{v}_{hd}}{\left(\mu_{EOF} + \mu_{ep1}\right) E\cos\varphi + \overline{v}_{hd}} \right) \times \\ \left(\left(\mu_{EOF} + \frac{\mu_{ep1}\overline{v}_{hd}}{\left(\mu_{EOF} + \mu_{ep1}\right) E\cos\varphi + \overline{v}_{hd}} \right) \left(\frac{1}{2} - \frac{\Lambda}{5} - \frac{\Gamma_1}{3} \right) \right. \\ \left. -\mu_{ep1} P_1 \frac{\mu_{EOF} E\cos\varphi + \overline{v}_{hd}}{\left(\mu_{EOF} + \mu_{ep1}\right) E\cos\varphi + \overline{v}_{hd}} \right) \\ + D_1 \left(1 + \left(\frac{\mu_{ep1} E\sin\varphi}{\left(\mu_{EOF} + \mu_{ep1}\right) E\cos\varphi + \overline{v}_{hd}} \right)^2 \right) \end{array} \right)} + \right.$$

$$\left. \sqrt{\frac{w_0^{\,2}}{12} + \frac{2L}{\left(\mu_{EOF} + \mu_{ep2}\right) E\cos\varphi + \overline{v}_{hd}} \left(\begin{array}{l} \frac{h^2 E^2 \sin^2\varphi}{105 D_2} \left(\mu_{EOF} + \frac{\mu_{ep2}\overline{v}_{hd}}{\left(\mu_{EOF} + \mu_{ep2}\right) E\cos\varphi + \overline{v}_{hd}} \right) \times \\ \left(\left(\mu_{EOF} + \frac{\mu_{ep2}\overline{v}_{hd}}{\left(\mu_{EOF} + \mu_{ep2}\right) E\cos\varphi + \overline{v}_{hd}} \right) \left(\frac{1}{2} - \frac{\Lambda}{5} - \frac{\Gamma_2}{3} \right) \right. \\ \left. -\mu_{ep2} P_2 \frac{\mu_{EOF} E\cos\varphi + \overline{v}_{hd}}{\left(\mu_{EOF} + \mu_{ep2}\right) E\cos\varphi + \overline{v}_{hd}} \right) \\ + D_2 \left(1 + \left(\frac{\mu_{ep2} E\sin\varphi}{\left(\mu_{EOF} + \mu_{ep2}\right) E\cos\varphi + \overline{v}_{hd}} \right)^2 \right) \end{array} \right)} \right) \tag{4.20}$$

A more explicit form of Equation (4.20) is possible, but its sheer size prevents us from presenting it here. Instead we recommend that the values of Λ, Γ, and P be calculated directly using Equations (3.21), (3.33) and (4.3) respectively:

$$\Lambda = \frac{\alpha_\eta \kappa E^2 h^2}{8\lambda}, \quad \Gamma = \frac{\alpha_{D_i} \kappa E^2 h^2}{8\lambda}, \quad P = \frac{\alpha_{\mu_i} \kappa E^2 h^2}{8\lambda}, \quad i = 1, 2 \tag{4.21}$$

For analytes 1 and 2, the parameters Γ and P are different, as reflected by their subscripts in Equation (4.20).

The combined influences of Λ, Γ, and P are not obvious. Viscosity decreases as the temperature of the electrolyte increases and changes in viscosity lead to increased dispersion. Diffusion increases with increasing temperature so that differences in concentration as a function of z are reduced by small increases in temperature. Differences in electrophoretic mobility with z actually lead to a slight reduction in dispersion for small temperature differences provided that the directions of the electroosmotic mobility and electrophoretic mobility are opposite at $z = 0$. In such cases, the parabolic profile of electrophoretic velocity due to temperature variations in the z direction are partly balanced by the oppositely shaped profile of the electroosmotic velocity due to recirculation at the side walls. This idea is illustrated as a schematic in Figure 3 below:

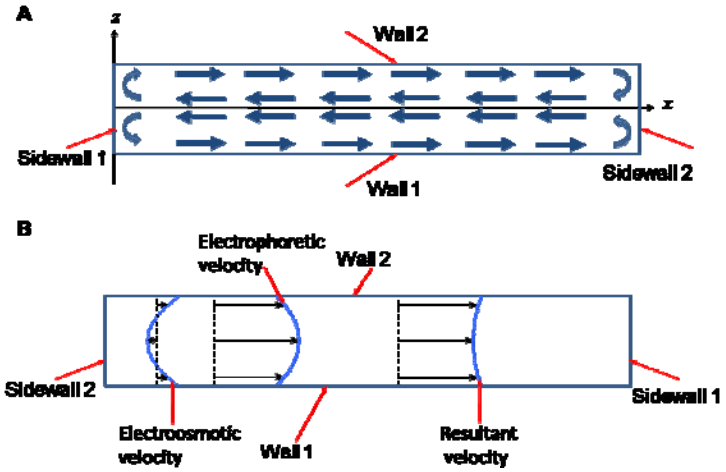

Figure S-3 Schematic illustration of the recirculation of the electroosmotic flow in the *x*-*z* plane (**A**) and the fact that the opposing velocity profiles of the electroosmotic velocity and the electrophoretic velocity may result in an overall decrease in hydrodynamic dispersion. (Diagram adapted from Strickler and Sacks[3])

It should be noted that for ΔT > 1ºC, buoyancy effects due to differences in density of the electrolyte produce convection currents which lead to a substantial increase in dispersion. These effects have not been taken into account in our general equation.

III. Comparison with previous expressions for resolution

A most interesting difference between Equation (4.19) and earlier expressions for µFFE, is that for some conditions, peak broadening decreases significantly when:

$$\mu_{\mathrm{EOF}} E_x + \frac{\overline{v}_{1,x}}{\overline{v}_{1,y}} \overline{v}_{\mathrm{hd}} \approx 0 \tag{5.1}$$

This effect is well-known in macro-FFE;[3,9] the electroosmotic mobility is adjusted by matching the zeta-potential of the wall to the zeta-potential of one of the particles to be separated to reduce its bandwidth. To the best of our knowledge, this approach for maximising resolution has not been described for µFFE.

It should be noted that our equation for resolution purposefully does not contain any transient adsorption effects, described by Raymond et al.,[10] as this effect only exists in non-stationary conditions; we have assumed that after a period of "equilibration", the processes of adsorption and desorption from the walls fully compensate each other.

It is informative to compare Equation (4.19) with previous expressions for resolution in µFFE. In 2006, Fonslow and Bowser published an equation for resolution that considered sample injection, diffusional band broadening and hydrodynamic broadening.[11] Using our notation, their equation can be rewritten as:

$$R_{\mathrm{S}} = \frac{\left|\left(\mu_{\mathrm{ep1}} - \mu_{\mathrm{ep2}}\right) EL\right|}{2\overline{v}_{\mathrm{hd}} \left(\sqrt{\frac{w_0^{\,2}}{12} + \frac{2D_1 L}{\overline{v}_{\mathrm{hd}}} + \frac{h^2 \left(\mu_{\mathrm{ep1}} + \mu_{\mathrm{EOF}}\right)^2 E^2 L}{105 D_1 \overline{v}_{\mathrm{hd}}}} + \sqrt{\frac{w_0^{\,2}}{12} + \frac{2D_2 L}{\overline{v}_{\mathrm{hd}}} + \frac{h^2 \left(\mu_{\mathrm{ep2}} + \mu_{\mathrm{EOF}}\right)^2 E^2 L}{105 D_2 \overline{v}_{\mathrm{hd}}}} \right)} \tag{5.2}$$

Obviously, the first major difference between our equation for resolution, Equation (4.19), and their version is the inclusion of a variable angle between E and v_{hd}. Its inclusion opens up new opportunities for increasing resolution. By reducing the hydrodynamic velocity so that the apparent electrophoretic velocities (= v_{ep} + v_{EOF}) of the separated streams are just smaller than v_{hd}, and by adjusting φ so that $v_y \approx 0$ for the

stream of molecules with the larger electrophoretic mobility, resolution can be increased significantly relative to orthogonal μFFE. The mechanism for this improved resolution is that the products spend different amounts of time in the electric field so that the lateral displacement of the species with the greater electrophoretic mobility is significantly enhanced.

Another major difference between our equation and Equation (5.2) can be observed by setting φ equal to 90º in Equation (4.19) allowing us to compare the orthogonal case. The last term in both Equations (4.15) and (4.16) describes the effects of diffusion in the direction of the hydrodynamic flow. This source of band broadening was completely overlooked by previous authors. Our more comprehensive equation for resolution in orthogonal μFFE, which includes diffusion in the direction of the hydrodynamic flow (3rd and 7th terms in denominator), is shown below:

$$R_S = \frac{\left|\left(\mu_{ep1} - \mu_{ep2}\right) LE\right|}{2\overline{v}_{hd}\left(\sqrt{\frac{w_0^2}{12} + \frac{2D_1 L}{\overline{v}_{hd}} + \frac{2D_1 L \mu_{ep,1}{}^2 E^2}{\overline{v}_{hd}{}^3} + \frac{h^2\left(\mu_{EOF} + \mu_{ep1}\right)^2 E^2 L}{105 D_1 \overline{v}_{hd}}} + \sqrt{\frac{w_0^2}{12} + \frac{2D_2 L}{\overline{v}_{hd}} + \frac{2D_2 L \mu_{ep2}{}^2 E^2}{\overline{v}_{hd}{}^3} + \frac{h^2\left(\mu_{EOF} + \mu_{ep2}\right)^2 E^2 L}{105 D_2 \overline{v}_{hd}}}\right)} \tag{5.3}$$

Generally, at flow rates required to achieve the maximum resolution in orthogonal FFE, the variance associated with diffusion in the y direction is of a similar magnitude to the variance associated with diffusion in the x direction. Inspection of Equation (5.3) shows that at very low flow rates, diffusion in the y direction becomes the dominant source of band broadening.

IV. Conditions used in computer simulations in Figure 3 in main text

Diffusion coefficients and electrophoretic mobilities were calculated using the Stokes-Einstein equation[12] for two species each with a charge of Z = +2, density of 1.2 g/mL, and MW ~ 1 kDa, which differ in mass by 14 Da. The calculated electrophoretic mobilities were: $\mu_{ep1} = 2.753 \times 10^{-8}$ m^{2}s^{-1}V^{-1} and $\mu_{ep2} = 2.766 \times 10^{-8}$ m^{2}s^{-1}V^{-1} respectively. The hydrodynamic flows for the separation of the products were adjusted so that the average widths of the streams after separation would be the same in **A** and **B**. In **A**, $\overline{v}_{hd} = 6.21 \times 10^{-5}$ ms^{-1} and for **B**, $\overline{v}_{hd} = 5.60 \times 10^{-4}$ ms^{-1}. The magnitude of the electrical field strength was the same in **A** and **B,** $E = 2.0 \times 10^4$ Vm^{-1} but the angle, φ, was different. In **A**, φ = 90º and in **B**, φ = 177.1º. The height of the separation channel was assumed to be 20 μm for both **A** and **B**. The electrolyte, 25 mM HEPES (4-(2-hydroxyethyl)-1-piperazineethanesulfonic acid) adjusted to a pH = 7.00 using NaOH, had a calculated electrical conductivity of 0.043 Sm^{-1}. The electroosmotic flow was assumed to be negligible as was the temperature difference in the channel due to Joule heating. The latter assumption was verified using an equation derived by Ravoo.[5] According to Ravoo, the maximum temperature difference in the electrolyte is given by:

$$\Delta T_{max} = \frac{\kappa E^2 h^2}{8\lambda} \tag{6.1}$$

Using the experimental conditions described and $\lambda = 0.605$ Wm^{-1}K^{-1} for the thermal conductivity of water, the expected rise in temperature is 1.42×10^{-3} K, so that each of the parameters, Λ, Γ and P are smaller than 0.004% and can legitimately be ignored.

References

1. Taylor, G. *P. Roy. Soc. Lond. A Mat.* **1954**, *A225*, 473-477
2. Aris, R. *P. Roy. Soc. Lond. A Mat*. **1956**, *A235*, 67-77
3. Strickler, A.; Sacks, T. *Ann. N.Y. Acad. Sci.* **1973**, *209*, 497-514
4. Gill, W.N., Sankarasubramanian, R. *P. Roy. Soc. Lond. A Mat*. **1970,** *A316,* 341-350
5. Ravoo, E.; Gellings, P. J.; Vermeulen, T. *Anal. Chim. Acta* **1967**, *38*, 219-232.
6. Kirby, B. J.; Hasselbrink, E. F. J. *Electrophoresis* **2004**, *25*, 187-202.

7. Evenhuis, C.J.; Hruska, V.; Guijt, R.M.; Macka, M.; Gas, B.; Marriott, P.J.; Haddad, P.R. *Electrophoresis,* **2007**, *28*, 3759-3766.
8. Harris, D.C. *Quantitative Chemical Analysis,* 4th ed.*;*W.H Freeman and Company: New York, 1995
9. Hannig, K.; Wirth, H.; Meyer, B-H.; Zeiller, K. *H- S. Z. Physiol. Chem.*, **1975**, *356*, 1209-1223.
10. Raymond, D. E.; Manz, A.; Widmer, H. M. *Anal. Chem.* **1996**, *68*, 2515-2522.
11. Fonslow, B. R.; Bowser, M. T. *Anal. Chem.* **2006**, *78*, 8236-8244
12. Kaiser, T.J.; Thompson, J.W.; Mellors, J.S.; Jorgenson, J.W. *Anal. Chem.* **2009**, *81*, 2860-2868.